ELSEVIER

Cardiovascular Research 64 (2004) 72–83

Cardiovascular Research

www.elsevier.com/locate/cardiores

Mechanisms of heart failure with well preserved ejection fraction in dogs following limited coronary microembolization

Kun-Lun He[a,*], Marc Dickstein[b], Hani N. Sabbah[c], Geng-Hua Yi[d], Anguo Gu[d], Mathew Maurer[d], Chi-Ming Wei[e], Jie Wang[d], Daniel Burkhoff[d]

[a] *Department of Cardio-Nephrology, Chinese PLA General Hospital, 28 Fuxing Road, Beijing 100853, China*
[b] *Division of Anesthesiology, College of Physicians and Surgeons of Columbia University, New York City, NY 10032, USA*
[c] *Division of Cardiovascular Medicine, Henry Ford Heart and Vascular Institute, Henry Ford Health System, Detroit, MI 48202, USA*
[d] *Division of Circulatory Physiology, College of Physicians and Surgeons of Columbia University, New York City, NY 10032, USA*
[e] *Department of Surgery, University of Maryland School of Medicine, Baltimore, MD 21201, USA*

Received 16 January 2004; accepted 7 June 2004
Available online 21 July 2004
Time for primary review 19 days

Abstract

Objective: It has been suggested that in some settings, heart failure (HF) may occur with normal ejection fraction (EF) as a consequence of undetected systolic dysfunction. However, others have argued that this can only occur in the presence of diastolic dysfunction. We therefore sought to determine the contribution of diastolic dysfunction in an animal model of HF with normal EF. **Methods and results:** Limited myocardial injury was induced in 21 dogs chronically instrumented to measure hemodynamics and LV properties by daily coronary microembolization (~ 115 μm beads) until LV end diastolic pressure (LVEDP) was ≥ 16 mm Hg. Nine dogs developed HF within 16 ± 6 days (LVEDP 12 ± 2 vs. 21 ± 2 mm Hg, $p < 0.001$) with no significant change in dP/dt_{max} (2999 ± 97 vs. 2846 ± 189 mm Hg/s), mean arterial pressure (103 ± 4 vs. 100 ± 4 mm Hg), EF (57 ± 5% vs. 53 ± 4%) or E_{es} (end-systolic elastance, 3.1 ± 0.9 vs. 2.9 ± 0.8 mm Hg/ml) but with an ~ 10 ml increase in V_o (14 ± 12 vs. 25 ± 16 ml; $p < 0.01$). The EDPVR and time constant of relaxation (τ, 25 ± 3 vs. 28 ± 3 ms) did not change significantly. These animals were hemodynamically stable out to 3 1/2 months. Neurohormonal activation occurred (elevations of NE, AngII, BNP) and there was intravascular volume expansion by ~ 16% ($p < 0.05$). **Conclusions:** A small amount of myocardial injury can lead to neurohormonal activation with intravascular volume expansion and elevation of LVEDP in the absence of reductions in dP/dt_{max} or EF and without diastolic dysfunction. Thus, HF with preserved EF does not a priori equate with *diastolic heart failure*.

Keywords: Heart failure; Diastole; Autonomic nervous system; Pressure–volume relationships

This article is referred to in the Editorial by P. Steendijk (pages 9–11) in this issue.

1. Introduction

Chronic heart failure (CHF) in the setting of normal left ventricular ejection fraction (EF) is a common finding in a variety of clinical settings such as hypertension and prior myocardial infarction [1,2]. Since systolic function is considered normal, the mechanism of CHF is typically ascribed to an abnormality of diastolic function, leading to the diagnosis of "diastolic heart failure." For patients with small myocardial infarcts in particular, it has been proposed that CHF develops as a result of myocardial hypertrophy and interstitial fibrosis which in turn increases myocardial wall stiffness and impairs active relaxation [3–5]. Consequently, high LV filling pressures are required to maintain normal (or near normal) filling volumes and cardiac output, which leads to heart failure. Although widely accepted, it has never been proven that this explains chronic heart failure with normal ejection fraction in the post-infarction setting. However, other groups have suggested that in some settings, heart failure may occur with normal ejection

* Corresponding author. Tel.: +86-10-68152720; fax: +86-10-67089714.
E-mail address: hekunlun2002@yahoo.com (K.-L. He).

0008-6363/$ - see front matter © 2004 European Society of Cardiology. Published by Elsevier B.V. All rights reserved.
doi:10.1016/j.cardiores.2004.06.007

fraction as a consequence of undetected systolic dysfunction alone or in combination with diastolic dysfunction [6,7]. In view of the relatively indirect nature of the noninvasive measures used to quantify systolic function in the clinical setting on which these conclusions are based, this remains a controversial matter.

Repeated coronary artery embolizations with microspheres has been shown to result in systolic heart failure (SHF) with chamber dilation in dogs, mimicking ischemic cardiomyopathy in humans [8,9]. Histologic analysis of the myocardium reveals a mixture of dense transmural infarcts, increased interstitial fibrosis and myocyte hypertrophy. We hypothesized that use of fewer embolizations, and therefore induction of a smaller amount of myocyte loss, would lead to interstitial fibrosis, "diastolic dysfunction" and CHF with preserved global LV systolic performance. In this experimental setting, ventricular systolic and diastolic properties could be measured accurately and repeatedly over time. Using this approach, we set out to test the hypothesis that heart failure can be created with clinically undetectable left ventricular dysfunction and to determine the degree to which diastolic dysfunction and other factors contribute to generation of the CHF state.

2. Methods

2.1. Surgical preparation

Twenty one mongrel dogs (27–35 kg) which formed the main part of this study were chronically instrumented for hemodynamic measurements and repeated coronary microembolization as detailed previously [8]. After anesthesia (isoflurane 1–2%), initiation of mechanical ventilation and thoracotomy, animals were instrumented with Tygon catheters (Cardiovascular Instruments, MA) in the descending thoracic aorta and LV, a solid-state pressure gauge (P6.5, Konigsberg Instruments, Pasadena, CA) through the LV apex, a silicon catheter in the proximal left anterior descending coronary artery (LAD) and intercommunicating subepicardial sonomicrometer crystals (Sonometrics, London, Ontario) for measurement of anterior–posterior, septal-free wall and apex-base dimensions. An inferior vena caval pneumatic occluder was implanted for transient reduction of ventricular filling. Catheters and wires were externalized through the back. After full recovery, dogs were trained to lie quietly on a laboratory table. CHF was induced by daily injections of 25,000–50,000 polystyrene microspheres (Bangs Laboratories, IN; 98–115 μm diameter) through the implanted LAD catheter until LV end-diastolic pressure (LVEDP) was $\geq$18 mm Hg.

Four additional dogs underwent multiple coronary embolizations by repeated femoral arterial cut-downs [9]. After establishment of the CHF, these animals were instrumented with LV and aortic pressure transducers and were studied over a 3–4 month period.

2.2. Experimental design and protocol

For the 21 dogs of the main part of the study, hemodynamic measurements were obtained at baseline, weekly until CHF (LVEDP $\geq$18 mm Hg) was achieved and 2.5 ± 0.7 weeks after establishment of CHF. Plasma neurohormone values and total blood volume were measured in a subset of these dogs as detailed below. In these animals and in the four additional animals, standard echocardiographic imaging (SONOS 5500, Agilent Technologies) was performed for quantification of chamber dimensions and area EF at the basal, mid-papillary and apical levels and global EF estimated according to the methods of Dubroff et al. [10]. All measurements described above were made with animals in an awake state without any sedation and after a minimum of 30 min acclimation to being placed on the table.

2.3. Pressure–volume analyses

During hemodynamic studies, the inferior vena cava was transiently occluded with the pneumatic occluder in order to obtain a family of pressure–volume curves spanning a range of loading conditions to determine pressure–volume relationships. LV volumes (LVV) were estimated from LV sonomicrometrically measured dimensions assuming an ellipsoid model: $LVV = \pi AP \cdot SF \cdot AB/6$, where AP is anterior–posterior, SF is septal-free wall, and AB is apex-base dimensions. Since the crystals were placed in a subepicardial position, the volume determined from these dimensions is the sum of the intracavitary volume plus myocardial volume which, based upon echocardiographic measurements, did not vary significantly during the course of the experiment. The end-systolic and end-diastolic pressure–volume points were determined for beats at end-expiration in the usual fashion. Linear regression analysis used to determine the slope (E_{es}) and volume axis intercept (V_o) of the end-systolic pressure–volume relationship (ESPVR) [11,12]. Systolic properties were also assessed by preload-recruitable stroke work (PRSW) [13] which was characterized by the slope (M_{PRSW}) and volume-axis intercept (M_o) of the end-diastolic volume–stroke work relationship.

The end-diastolic pressure–volume relationship (EDPVR) was determined by applying non-linear regression analysis to the end-diastolic pressure and volume points (P_{ed} and V_{ed}, respectively). These data were fit to the following two equations: $P_{ed} = P_o + be^{aV_{ed}}$ and $P_{ed} = be^{aV_{ed}}$ (the second expression simply eliminating the P_o term). The reason for using both equations is that the former equation is more widely used and can account for changes in the EDPVR asymptote. When the data range includes only positive end-diastolic pressures, the simpler equation typically fits the data equally well and has the advantage that it can be linearized by logarithmic transformation so that comparisons of relations measured at different time points and/or between

groups can be accomplished by analysis of covariance (discussed further below). In addition to fitting and assessing for changes in actual EDPVRs, the data were also used to assess chamber and myocardial stiffness constants as detailed in prior studies [14,15]. To calculate a unitless chamber stiffness constant (α), ventricular volume was normalized to myocardial wall volume (V_w) and the data then fit to the following equation: $P_{ed} = \beta e^{\alpha V_{ed}/V_w}$. For this purpose, V_w is estimated from the echocardiographic determinations of wall thickness and chamber diameter using a spherical model. To calculate a unitless myocardial stiffness constant (μ), the relationship between midwall radius (R_m) and diastolic wall stress (σ) is fit to the equation: $\sigma = \lambda R_m^3 \mu$. The equations used to estimate midwall radius and wall stress have been summarized previously [15].

Arterial afterload was also quantified via the pressure–volume approach using the effective arterial elastance, E_a [16]. This is estimated in the usual fashion as the ratio between end-systolic pressure and stroke volume (SV): $E_a P_{es}/SV$. SV was calculated as the difference between end-diastolic and end-systolic volumes determined under steady state conditions from the sonometrically determined volumes (i.e., prior to IVC occlusion) from the analysis defined above. As described previously, E_a is primarily determined by total peripheral resistance and heart rate (HR); in the setting of constant HR changes in E_a therefore reflect changes in TPR.

Active relaxation was quantified by the time constant of pressure fall (τ) by fitting the diastolic phase of the LV pressure wave (starting at dP/dt_{min}) and allowing a non-zero asymptote.

2.4. Measurement of total blood volume

Measurement of total blood volume was made using the BVA-100 blood analyzer (Daxor Corporation, New York). The procedure starts with the dogs lying on the table for a minimum of 30 min. After obtaining a 5-ml reference sample of venous blood, pre-mixed human albumin I^{131}-labeled (25 μCi) is administered. Starting 12 min later, five additional venous blood samples are obtained at 6-min intervals. Detected radiation intensity reflects the time course of mixing of I^{131} into the total blood volume and the BVA-100 calculates the total blood volume based on the time course of change in radiation [17].

2.5. Measurement of the plasma neurohormones

Blood samples were collected via the implanted aortic catheter at baseline, heart failure and the state of sustained heart failure with dogs resting quietly on the laboratory table for at least 20 min to determine the plasma levels of B-natriuretic peptide, angiotensin II, and norepinephrine. Commercially available radioimmunoassay (RIA) kits (Peninsular Laboratory, Belmont, CA, USA) were used.

2.6. Data analysis and statistics

All results are expressed as mean ± SD. Changes in hemodynamic parameters between pre- and post-heart failure values were compared using repeated measures analysis of variance (rmANOVA). Relations (ESPVR, PRSW, EDPVR) between various time points were compared using multiple linear regression analysis (MLRA). In the case of the EDPVR, $P_{ed} = be^{aV_{ed}}$ was linearized by logarithmic transformation [$\ln(P_{ed}) = \ln(b) + aV_{ed}$] so that MLRA could be applied to test for changes between conditions. The equations $P_{ed} = \beta e^{\alpha V_{ed}/V_w}$ and $\sigma = \lambda R_m^{3\mu}$ were similarly linearized [$\ln(P_{ed}) = \ln(\beta) + \alpha V_{ed}/V_w$ and $\ln(\sigma) = \ln(\lambda) + 3\mu \ln(R_m)$, respectively] for application of MLRA to determine changes in α and μ. Statistical significance was determined at $p < 0.05$ and p values were adjusted for multiple comparisons using a Bonferroni correction.

This study was approved by the Institutional Animal Care and Use Committee of the College of Physicians and Surgeons of Columbia University and the Henry Ford Health System. The investigation conforms with the *Guide for the Care and Use of Laboratory Animals* published by the US National Institutes of Health (NIH Publication No. 85-23, revised 1996).

3. Results

3.1. Baseline versus post-embolization hemodynamics

At baseline, LVEDP (11.3 ± 2.4 mm Hg), dP/dt_{max} (2980 ± 153 mm Hg/s, ranging between 2670 and 3320 mm Hg/s), LVSP (132 ± 8 mm Hg), mAoP (103 ± 5 mm Hg), heart rate (93 ± 11 bpm) and τ (25 ± 3 ms) measured from all 21 animals were within accepted normal limits. After 17 ± 5 days and an average of 826,000 ± 217,000 microspheres, EDP increased to an average of 20 ± 3 mm Hg in all dogs. However, the degree of EDP elevation did not correlate with the degree of systolic dysfunction, as evidenced by the lack of statistically significant correlation between EDP and dP/dt_{max} ($p = 0.12$, Fig. 1A). As shown in Fig. 1C, there was a reasonable correlation between dP/dt_{max} and echocardiographically determined ejection fraction (EF). As for dP/dt_{max}, post-embolization EF varied over a relatively wide range, including normal to mildly decreased values (between 40 and 60).

3.2. Subgrouping of animals

As illustrated by the data of Fig. 1, a wide range of hemodynamic responses was observed in response to the repeated coronary embolizations. In recognition of the fact that the goal of the present study was to understand the pathophysiologic mechanisms of the development of heart failure in the setting of preserved systolic function, we segregated a group of dogs that had heart failure yet had

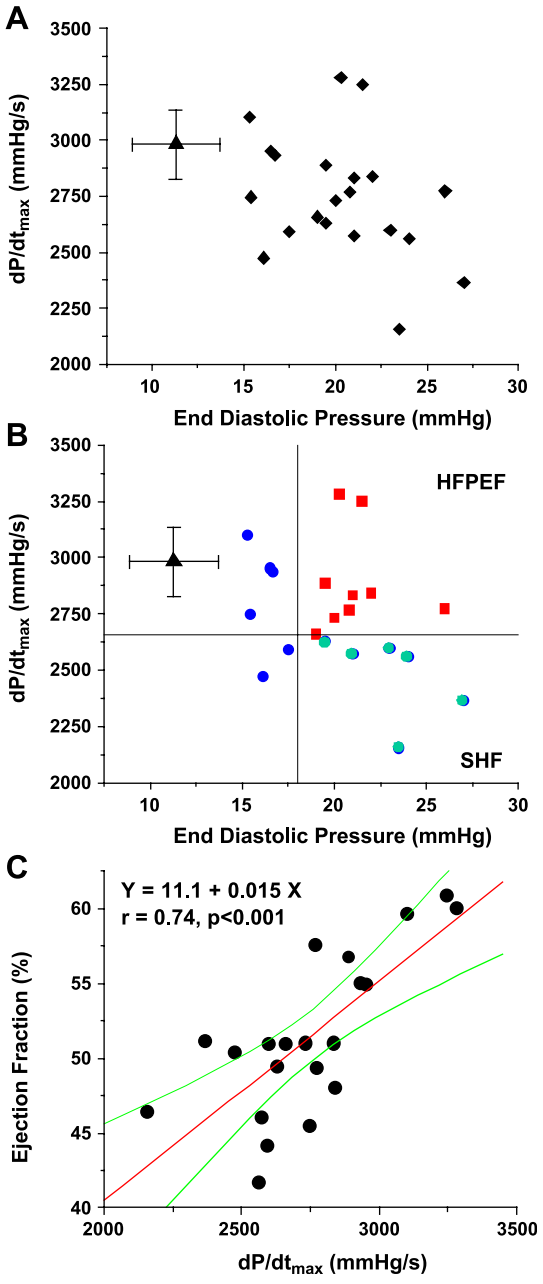

Fig. 1. (A) End-diastolic pressure (EDP) and maximal rate of pressure rise (dP/dt_{max}) following 17 ± 5 days of coronary microembolization (diamonds) show no overall correlation. The group mean ± SD normal baseline values shown by triangle. (B) Nine dogs (red circles) developed heart failure (EDP ≥ 18 mm Hg) with preserved systolic function (dP/dt_{max} within the normal range; HFPEF). Other animals developed heart failure with more significant reduction in dP/dt_{max} (green circles, $n = 6$) which where designated as the systolic heart failure (SHF) group. Still other animals (blue circles, $n = 6$) developed lesser degrees of EDP elevation. (C) There was a reasonably good correlation between dP/dt_{max} and ejection fraction at the onset of heart failure.

preserved systolic function. Heart failure was defined as an elevation of end-diastolic pressure to 18 mm Hg or greater; *preserved systolic function* was considered to be present if dP/dt_{max} was within the normal range observed under baseline conditions (between 2650 and 3220 mm Hg/s) and if EF was greater than 50%. As shown by the red circles in Fig. 1B, 9 of the 21 dogs fulfilled these criteria. In these dogs, EDP averaged 21 ± 2 mm Hg ($p < 0.001$ vs. baseline), dP/dt_{max} averaged 2846 ± 190 mm Hg/s (p = NS vs. baseline) and EF averaged 53 ± 4% (p = NS vs. baseline value of 57 ± 5%). Similar to the clinical scenario, these animals shall be designated as having heart failure with preserved ejection fraction (HFPEF).

In other dogs there was more significant depression of systolic function with increased EDPs, while in other animals there were relatively mild increases in EDP with or without significant changes in dP/dt_{max}. In particular, there were six animals with elevated EDP (23 ± 3 mm Hg, $p < 0.001$ vs. baseline), decreased dP/dt_{max} (2480 ± 183 mm Hg/s, $p = 0.005$ vs. baseline) and decreased ejection fraction 48 ± 4% ($p < 0.001$ vs. baseline); this group shall be designated as having mild systolic heart failure (SHF).

Overt signs of HF developed in 8 of the 9 HFPEF animals, including decreased food intake, weight loss, rapid respiratory rate, increased resting HR, pulmonary rales and ascites. Such signs were also present in all 6 of the animals that were designated as SHF. Interestingly, the number of

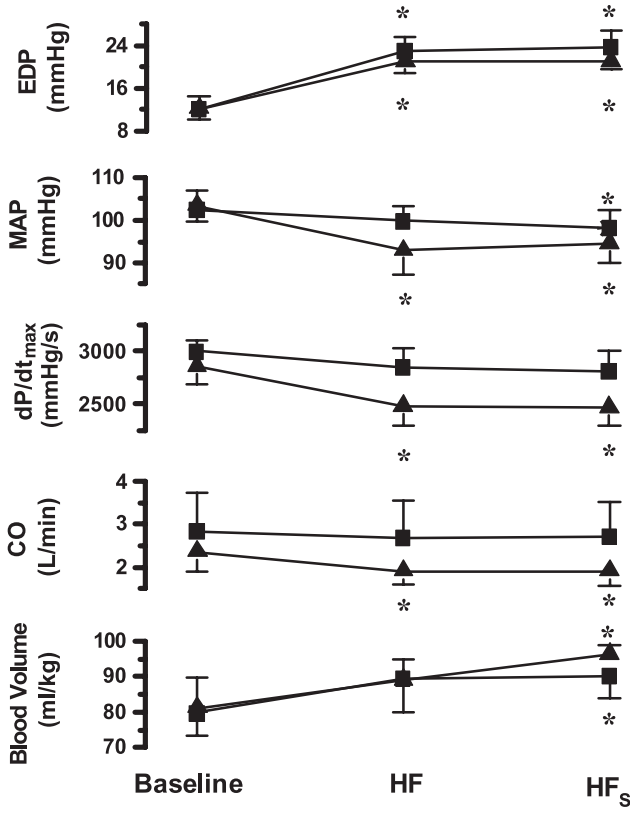

Fig. 2. End-diastolic pressure (EDP), mean arterial pressure (MAP), maximum rate of rise of pressure (dP/dt_{max}), cardiac output (CO) and total blood volume at baseline, at the onset of heart failure (17 ± 5 days of embolization) and with sustained heart failure (HFS, 2.5 ± 1.1 weeks after achieving the heart failure state). Animals with heart failure and preserved ejection fraction (HFPEF, $n = 9$) show by squares, while patients with more overt systolic heart failure (SHF, $n = 6$) shown by triangles. *$p < 0.05$ vs. baseline.

Table 1
Echocardiographic LV cross-sectional areas and EF at mid-papillary level at baseline, HF onset, and HF sustained in awake dogs with HFPEF and SHF

	Baseline	HF Onset	HF Sustained
Heart failure with preserved EF group (n = 7)			
Area			
EDA (cm^2)	15.2 ± 1.5	16.1 ± 1.9	16.5 ± 1.6
ESA (cm^2)	7.2 ± 0.7	8.2 ± 1.4	8.3 ± 1.1
Area EF (%)	52 ± 5	50 ± 3	49 ± 4
Global EF (%)	57 ± 5	53 ± 4	52 ± 6
Systolic heart failure group (n = 6)			
Area			
EDA (cm^2)	15.7 ± 1.5	17.4 ± 2.5*	17.2 ± 2.3*
ESA (cm^2)	8.1 ± 1.27	10.1 ± 1.6*	9.8 ± 1.5*
Area EF (%)	48 ± 6	41 ± 8*	43 ± 8*
Global EF (%)	55 ± 6	48 ± 4**	47 ± 10**

Values are means ± SD. EDA: end diastolic area; ESA: end systolic area; Area EF: area ejection faction. Global EF: global ejection fraction.
* Significantly ($p < 0.05$) different from Baseline.
** Significantly ($p < 0.01$) different from Baseline.

embolizations used to achieve the heart failure state did not differ significantly between the SHF and HFPEF groups ($7.5 \pm 2.7 \times 10^6$ microspheres over 16 ± 6 days vs. $8.7 \pm 1.6 \times 10^6$ microspheres over 19 ± 4 days, respectively, p = NS for both comparisons).

The criteria used for segregating the animals into the SHF and HFPEF groups, though objective, are arbitrary and not intended to imply clear dichotomy between groups. They are intended only to identify a group of animals which, by clinical criteria would unquestionably be considered to have heart failure and preserved systolic function.

3.3. Subgroup hemodynamics

Hemodynamics parameters for the two principal groups of animals at baseline, at the time of establishment of heart failure (HF) and ~ 2.5 weeks later (sustained heart failure state, HFs) are summarized in Fig. 2. In the HFPEF group (squares), LVEDP increased between baseline and HF state and there were no further significant changes over the ensuing 2.5 ± 1.1 weeks (HFs). Cardiac output was also preserved in this group. In the group of animals with more significant ventricular dysfunction, however (triangles), the rise in EDP was similar to that in the HFPEF group, but there were significant reductions in dP/dt_{max}, cardiac output and mean arterial pressure. Changes in cardiac output in this group were due to reductions in stroke volume since there was no significant change in heart rate. Measurements from the steady-state pressure–volume loops indicated that with

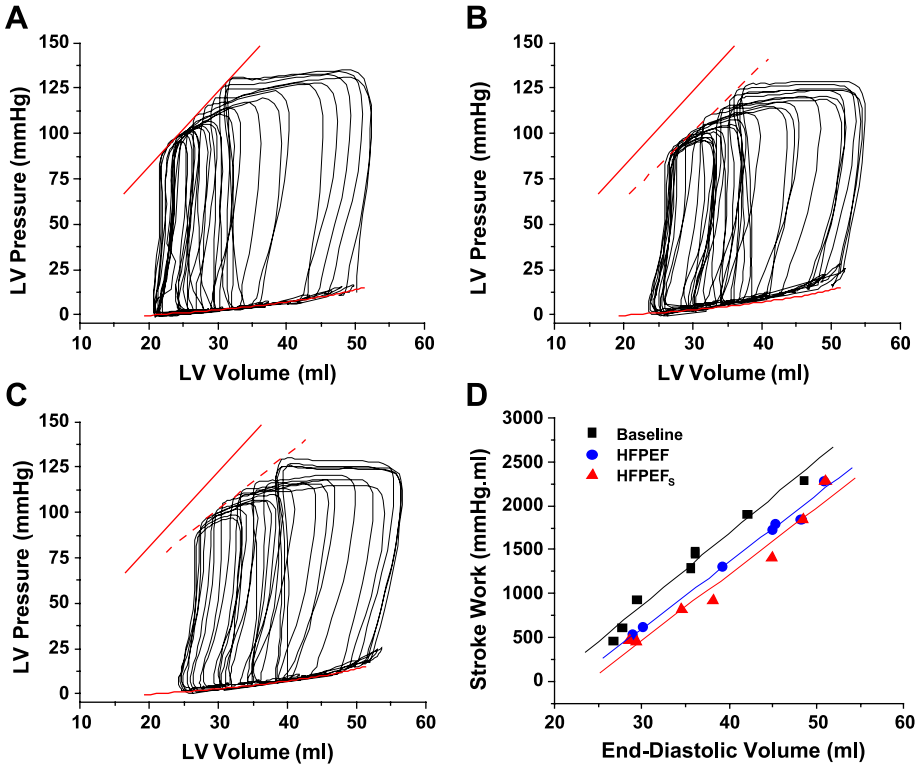

Fig. 3. Pressure–volume relationships obtained at baseline (A), ~ 2 weeks later after establishment of heart failure state (B) and ~ 3 weeks after establishing heart failure (C) in a representative animal. There is a small but significant rightward shift of the end-systolic pressure–volume relationship after establishment of heart failure which is sustained during the follow-up period (C). There is also a small upward shift of the end-diastolic pressure–volume relationship which is not sustained during the follow-up period. Similarly, the relationship between end-diastolic volume and stroke work (D, preload-recruitible stroke work) does not change slope, but is slightly shifted towards larger volumes.

the elevation of end-diastolic pressure, sonomicrometricly determined end-diastolic volume (which is the sum of intracavitary volume plus myocardial volume since the crystals were placed in a subepicardial position) increased in the HFPEF group from 93 ± 29 ml at baseline to 103 ± 29 ml at the onset of HF, to 106 ± 37 ml in the HFs state (each $p < 0.01$ versus baseline). In the SHF group, end-diastolic volumes increased similarly from a baseline value of 86 ± 17 to 97 ± 21 at the onset of HF to 101 ± 21 in HFs state ($p = 0.004$). End-systolic volumes also increased in both groups from the baseline, to HF and to HFs states (HFPEF: 61 ± 22 to 73 ± 24 to 76 ± 27, $p < 0.01$; SHF: 56 ± 11, 72 ± 16, 75 ± 16, $p < 0.01$).

Arterial afterload, quantified as the effective arterial elastance (E_a) was similar in HFPEF and SHF groups at baseline (5.7 ± 1.6 vs. 5.4 ± 1.5 mm Hg/ml). This value was unchanged over time in the SHF group (5.5 ± 1.7 and 5.7 ± 0.9 at HF and HFs, respectively). However, in the HFPEF group, the value decreased to 4.9 ± 1.1 and 4.8 ± 1.3 ($p = 0.02$) at HF and HFs timepoints.

3.4. Echocardiographic assessment

Compared to baseline, anterior–posterior and septum-free wall dimensions at the mid papillary level increased after establishment of heart failure in the HFPEF group so that cross-sectional areas also tended to increase, but this was not a statistically significant change (Table 1, $p = 0.08$). Neither fractional shortening nor area EF decreased significantly. There were also no changes in LV diastolic wall thickness over time which averaged ~ 1.05 cm in all cases. Similar results were obtained from the basal level. In the apical level, the region receiving the highest concentration of microspheres, there was a decrease in area EF from 47 ± 5% to 43 ± 5 % ($p = 0.03$ vs. baseline) in HF state and to 42 ± 7 in HFs. Global EF was not significantly reduced from baseline at the onset of HF or at the final follow-up.

In contrast, SHF animals (Table 1, bottom) exhibited significant increases in mean end-systolic and end-diastolic cross-sectional areas at the mid-papillary level and there was a significant decrease in mean area EF at the onset of SHF, changes which were similar in other levels of the heart and which were maintained during the follow-up period.

Color Doppler assessment indicated no significant mitral regurgitation in any of the animals.

3.5. Pressure–volume relationships

Pressure–volume loops and relationships from an HFPEF animal are shown in Fig. 3. Compared to baseline (panel A), there was an approximately parallel, small rightward shift of the ESPVR and a slight upward shift of the EDPVR at the onset of CHF (panel B). The change in ESPVR was sustained over the ensuing 2.5 ± 1.1 weeks

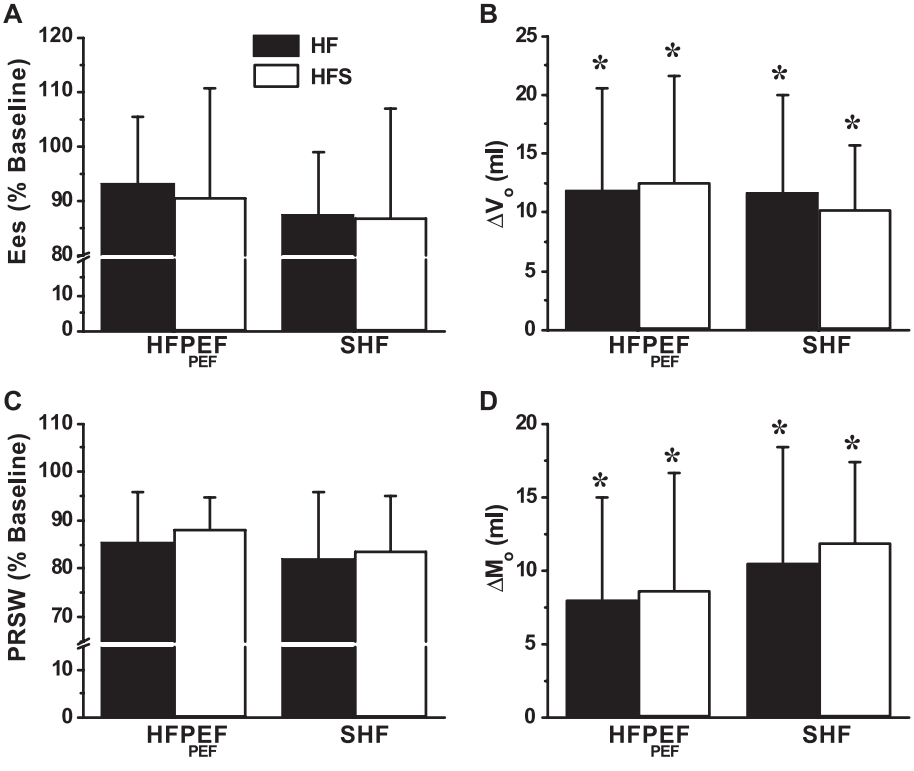

Fig. 4. End-systolic elastance (E_{es}, percent baseline), volume-axis intercept (V_o, changes from baseline), slope of preload recruitable stroke work (PRSW, percent baseline) and PRSW volume axis intercept (M_o, change from baseline) determined from ESPVR and PRSW, respectively, at the onset of heart failure and sustained heart failure state ($n = 9$ in HFPEF group and $n = 6$ in SHF group). *$p < 0.05$ by analysis of covariance. See text for details.

(panel C). PRSW behaved in a similar manner as the ESPVR (Panel D, no significant change in slope with rightward shift). The changes in EDPVR, however, were not sustained, consistent with chamber enlargement in the face of sustained elevation of EDP (discussed further below).

Parameter values characterizing ESPVR and PRSW over the course of the study are summarized in Fig. 4. As in the typical example, there were no significant changes in the ESPVR or PRSW slopes in HFPEF, but there were statistically significant ~10 ml rightward shifts (increases V_o and M_o by analysis of covariance). Statistically significant shifts of both ESPVR and PRSW were also detected at both follow-up time points in this group with no statistically significant change in E_{es}.

Original data and curve fits ($P_{ed} = be^{aVed}$) for EDPVRs from all HFPEF animals are shown in Fig. 5. Curve fits obtained using the three-parameter equation ($P_{ed} = be^{aVed}$)

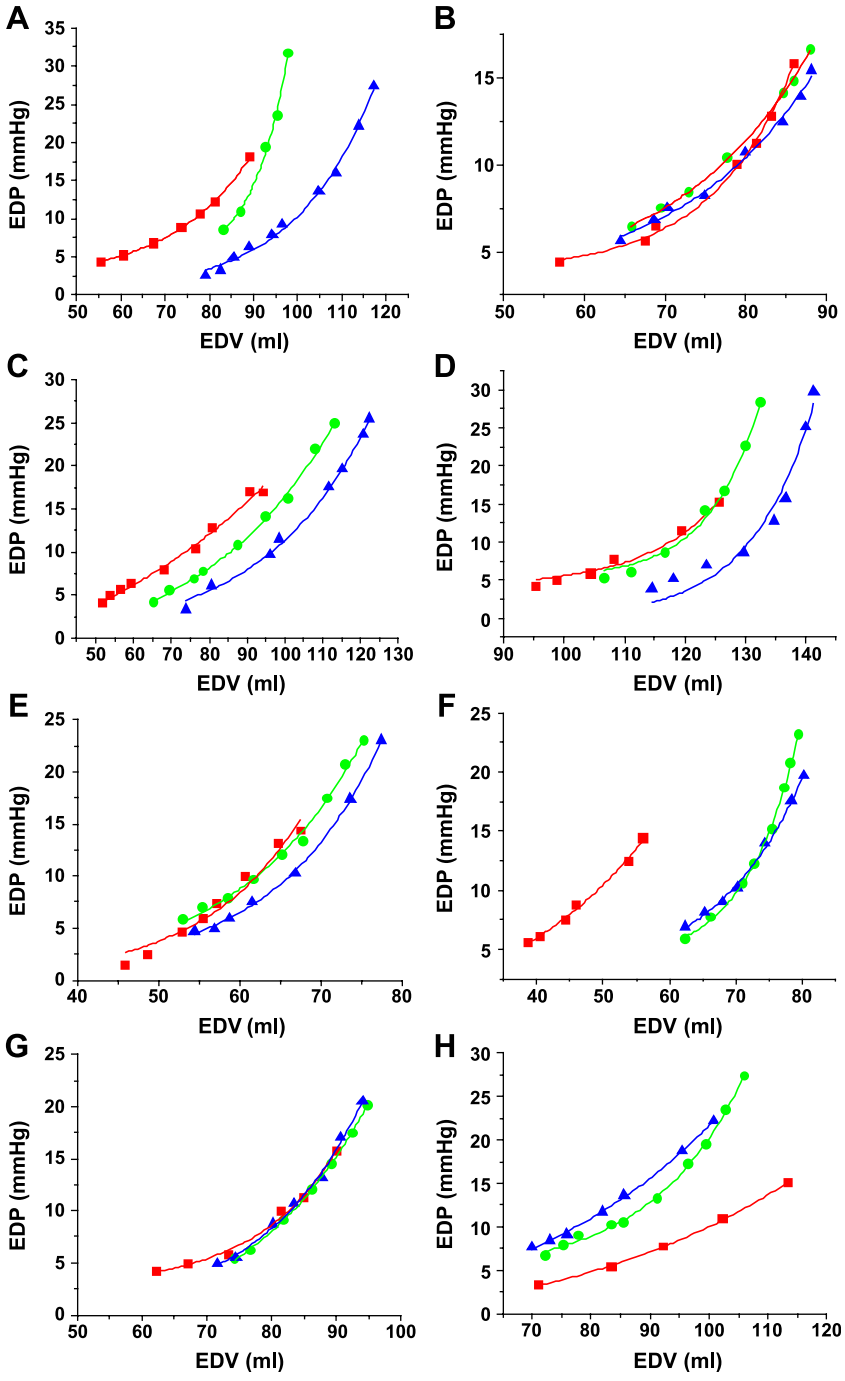

Fig. 5. End-diastolic pressure–volume relationships from all HFPEF hearts at baseline (red), onset of heart failure (green) and sustained heart failure state (blue). There is no consistent or significant change in these relations (analysis of covariance).

Table 2
End-diastolic pressure–volume analysis

Condition		$P_{ed}=P_o+b_1e^{a_1V_{ed}}$			$P_{ed}=b_2e^{a_2V_{ed}}$		Stiffness constant	
		P_o (mm Hg)	b_1 (mm Hg)	a_1 (1/ml)	b_2 (mm Hg)	a_2 (1/ml)	Chamber α (unitless)	Myocardial μ (unitless)
Baseline	Avg	−1.95	1.22	0.049	0.359	0.051	5.73	19.90
	SD	4.24	1.57	0.024	0.303	0.016	2.51	5.32
HFPEF ($n=9$)	Avg	1.00	0.26	0.072	0.216	0.064	7.12	25.54
	SD	2.70	0.42	0.027	0.211	0.021	2.68	8.14
$HFPEF_s$ ($n=9$)	Avg	0.76	0.27	0.069	0.255	0.059	6.03	23.70
	SD	2.20	0.51	0.035	0.255	0.019	1.86	7.64
Statistical Comparisons[a]								
Baseline vs. HFPEF		n/a			NS	NS	<0.01	NS
HFPEF vs. $HFPEF_s$		n/a			0.06	<0.005	0.003	NS
Baseline vs. $HFPEF_s$		n/a			NS	0.09	NS	NS

n/a, not applicable; NS, not significant.
[a] All p values determined by multiple linear regression analysis.

were equally good. Compared to baseline (red), EDPVRs measured after establishment of the heart failure state (green) were either similar to (panels B, D, E and G), shifted slightly upward or steeper (panels A and H) or slightly rightward shifted (panels C and F). Note, as seen in Fig. 3, that the resting baseline pressure–volume loop sits on each EDPVR at the highest point on each curve. It is important to note that in the HF state, the curves extend to higher volumes (as detailed above), a consequence of the increased filling pressure; thus, the steeper appearance of some (though not all) of these curves simply reflects this higher filling pressure on an intrinsically nonlinear curve. Compared to the HF state, the EDPVRs from the HFS state (blue) were similar to (panels B, F, G and H) or slightly right shifted (A, C, D and E) and spanned similar pressure ranges. Mean parameter values obtained for the two equations used to fit the EDPVR data are summarized in Table 2. For the three-parameter equation, mean Po varied very little between states. Compared to baseline, mean values for b decreased and a increased in both HF states. These same offsetting trends where present in the mean values

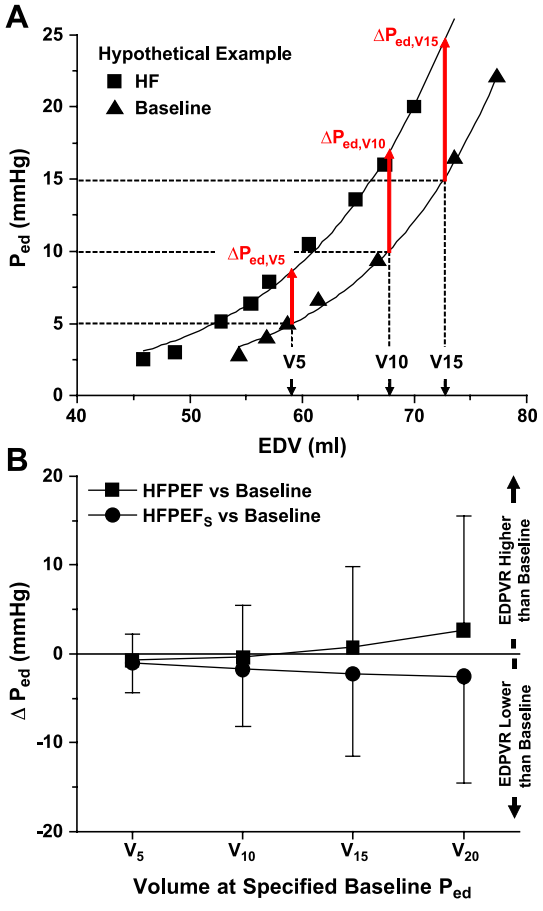

Fig. 6. A. The physiologic significance of changes in parameters of the EDPVR were assessed by determining changes in end-diastolic pressures changes from baseline (ΔP_{ed}) at volumes providing baseline end-diastolic pressures of 5, 10, 15 and 20 mm Hg (V_5, V_{10}, V_{15} and V_{20}, respectively). B. Mean changes in ΔP_{ed} at the specified volumes were small, with large standard deviations, consistent with lack of consistent changes in the EDPVR in HF and HFs states ($n=9$).

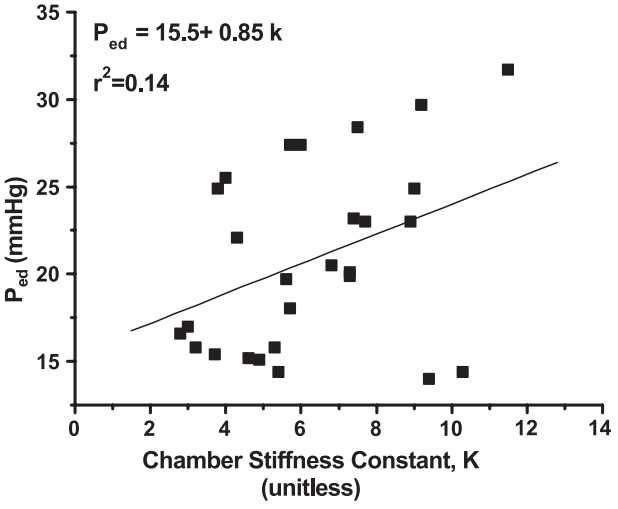

Fig. 7. No significant relationship existed between values of chamber stiffness constant and end-diastolic pressure (data from all nine HFPEF animals).

Table 3
Plasma neurohormonal levels (pg/ml) at baseline, HF onset, and HF sustained

	Heart failure with preserved EF ($n=6$)			Systolic heart failure ($n=5$)		
	Baseline	HF onset	HF sustained	Baseline	HF onset	HF sustained
Ang II	26.6 ± 7.4	38.3 ± 1.4	59.6 ± 8.8*	25.0 ± 17.9	41.3 ± 1.4	47.0 ± 8.8*
NE	189.0 ± 25.9	295.5 ± 44.3**	411.6 ± 80.2**	197.0 ± 25.9	281.0 ± 44.3**	402.0 ± 80.2**
BNP	13.4 ± 3.3	24.9 ± 11.5	26.0 ± 10.0*	11.2 ± 3.3	15.6 ± 11.5	23.9 ± 10.0**

Values are means ± SD. Ang II: Angiotensin II; NE: norepinephrine; BNP: B-Natriuretic.
* Significantly ($p<0.05$) different from Baseline.
** Significantly ($p<0.01$) different from Baseline.

of a and b in the two-parameter equation. The intrinsic covariance between these two parameters highlights the need for using multiple linear regression analysis to determine whether statistically significant shifts of the EDPVR exist between states. As summarized in the table, there was no statistically significant EDPVR shift between baseline and HF or HF_S. The statistical analysis indicated a difference in values for a between HF and HFs state (significance to be discussed further below). Compared to baseline, chamber stiffness constant (α) was increased at the onset of heart failure, but returned to baseline during the subsequent follow-up period. No change in myocardial stiffness constant (μ) was detected at either time point.

What is the meaning of changes in the parameter values noted above, and specifically, do they signify that diastolic dysfunction is the cause of the heart failure state. To explore these questions, two analyses were performed. The first was to assess on average how much was the EDPVR shifted in the HF and HF_S states, which was accomplished as follows. As shown in the hypothetical example in Fig. 6, Panel A, for each heart, the volume at which P_{ed} reached 5, 10, 15 and 20 mm Hg were determined from the baseline fits to the EDPVR. These volumes were designated V_5, V_{10}, V_{15} and V_{20}, respectively. At each of these volumes, the changes in pressure from baseline EDPVR to the EDPVR at one of the heart failure states (either HF or HF_S) were determined. These changes were designated $\Delta P_{ed,5}$, $\Delta P_{ed,10}$, $\Delta P_{ed,15}$ and $\Delta P_{ed,20}$, respectively, as shown in Panel A. Next, we determined average values for each of the ΔP_{ed} values and plotted them as a function of the volume (Panel B). As seen, the maximal average deviation from baseline occurred in each group at V_{20} and this amounted to only 2 mm Hg in the HF state and -2 mm Hg in the HFs state. There was no significant difference between groups at any volume. The standard deviations were relatively large in each group, consistent with the descriptions above indicating that in both groups that there were some instances where EDPVRs were either elevated, depressed or similar to baseline, but that there was no consistent change. This suggests that the development of heart failure was not tightly coupled with changes in the EDPVR.

To explore the meaning of changes in chamber stiffness constant, we examined the relationship between chamber stiffness constant and end-diastolic pressure (Fig. 7). As indicated by the data, there was a poor correlation between chamber stiffness and end-diastolic pressure.

Thus, a change in passive diastolic properties may or may not occur following a small amount of repeated coronary embolizations; increased chamber stiffness was not required for end-diastolic pressure to rise and increases in chamber stiffness were not proportionally related to increases in filling pressure.

3.6. Active relaxation

The time constant of relaxation (τ) varied very little between baseline (25 ± 3 ms), at the onset of heart failure (28 ± 3) or during subsequent follow-up (27 ± 2); τ did not differ between SHF and HFPEF groups.

3.7. Blood volume

Blood volume increased significantly from a baseline value of 80.4 ± 7.2 to 87.7 ± 6.7 ml/kg ($p=0.04$, $n=7$) after establishment of HFPEF (Fig. 2). This volume expansion increased further over the ensuing 2–3 weeks to 93.6 ± 5.2 ml/kg ($p=0.003$ vs. baseline). Similar intravas-

Table 4
Systemic hemodynamics during an average of 14.5 weeks follow-up in animals with HFPEF ($n=4$)

Weeks following HFPEF	LVSP (mm Hg)	LVEDP (mm Hg)	dP/dt_{max} (mm Hg)	MAP (mm Hg)	HR (bpm)
2.3 ± 0.2	127.0 ± 5.3	17.2 ± 4.0	2916.9 ± 169.3	101.5 ± 3.9	103 ± 13
8.0 ± 0.2	125.0 ± 4.1	17.7 ± 3.3	2893.8 ± 125.8	100.0 ± 3.5	102 ± 4
10.8 ± 0.2	125.4 ± 5.2	17.4 ± 2.0	2876.9 ± 119.9	100.3 ± 2.6	106 ± 20
14.5 ± 0.2	125.5 ± 5.2	17.8 ± 2.7	2885.5 ± 132.9	100.0 ± 3.9	107 ± 14

Values are means ± SD; $n=4$ dogs; LVEDP: left ventricular end diastolic pressure; LVSP: left ventricular systolic pressure; MAP: mean aortic pressure; HR: heart rate.

Table 5
Echocardiographic LV cross-sectional areas and EF at mid-papillary level during 14.5 weeks follow-up ($n=4$)

	HFPEF	HFPEF + 2 weeks	HFPEF + 7 weeks	HFPEF + 14.5 weeks
Diastole (cm^2)	14.6 ± 0.9	14.9 ± 0.7	14.7 ± 1.1	15.20 ± 0.9
Systole (cm^2)	7.6 ± 1.0	8.3 ± 0.99	8.2 ± 0.97	8.6 ± 1.1
Fraction (%)	48.4 ± 4.2	44.5 ± 4.6	44.2 ± 2.8	43.6 ± 4.4
Global EF (%)	52.9 ± 5.5	50.5 ± 4.7	48.4 ± 2.7	48.9 ± 5.0

Values are means ± SD; $n=4$ dogs.

cular volume expansion was noted in the SHF group (81.0 ± 8.7 at baseline, 96.1 ± 2.1 ml/kg at end of follow-up period; $p=0.02$ vs. baseline).

3.8. Plasma neurohormone levels

Plasma neurohormone levels, measured in 11 of the animals (6 in the HFPEF group) are summarized in Table 3. Compared to baseline, B-type natriuretic peptide, angiotensin II, and norepinephrine began increasing by the onset of HF and were each significantly elevated at the final observation period. There was no correlation between the changes in dP/dt_{max} or EF and elevations in neurohormone levels at the time of the onset of heart failure or 2 weeks later.

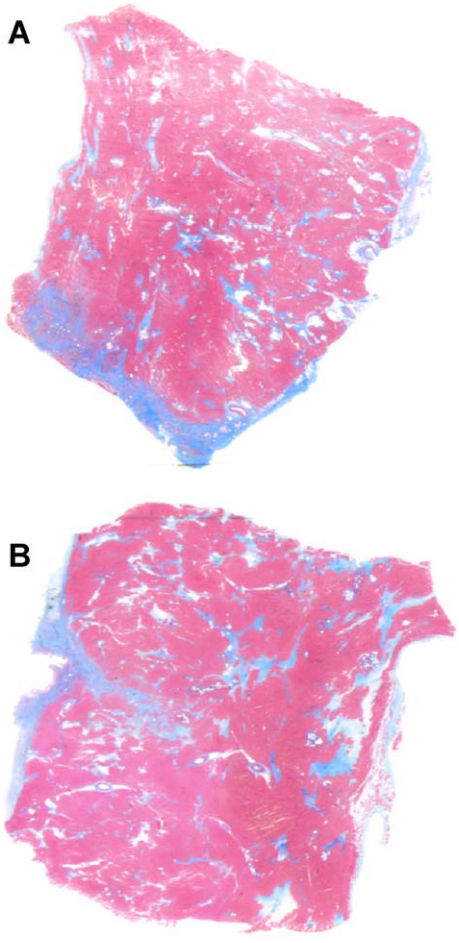

Fig. 8. Trichrome stained histologic sections taken from the anterior wall of animals surviving ~ 5 week (A) and ~ 4 months (B) showing transmural interstitial fibrosis.

3.9. Long term follow-up

A state of elevated EDP with preserved dP/dt_{max} and ejection fraction (HFPEF) was induced in four dogs by an average of 6.3 ± 3.4 percutaneous coronary microembolizations and 923,750 ± 76,000 microspheres. These animals were followed for an average of 3.6 months after induction of HFPEF. Systemic hemodynamics and echocardiographic data from these animals are summarized in Tables 4 and 5. Once HFPEF was induced, there were no significant changes in either hemodynamic or echocardiographic parameters (including anterior–posterior and septal-free wall dimensions, data not shown) over the follow-up period. These data indicate that these animals exhibit a relatively stable heart failure state over at least an average of 3.6 month timeframe.

3.10. Histology

Trichrome stained histologic sections taken from the anterior wall of animals surviving ~ 5 week (A) and ~ 4 months (B) are shown in Fig. 8. In both cases, the images reveal regions of transmural, diffuse interstitial fibrosis in the areas of microsphere injections. No acute inflammation was present.

4. Discussion

Delivery of a relatively small amount of coronary microembolizations, mimicking a small myocardial infarction, can generate heart failure (elevated EDP) with preserved systolic function as indexed by clinically used parameters such as EF and LV dP/dt_{max}. These animals demonstrated neurohormonal activation and expansion of intravascular blood volume and most developed overt signs of heart failure (rales, rapid respiratory rate, poor appetite, loss of weight, and ascites). Once established, the heart failure state was stable over a 5–15 week follow-up period.

Pressure–volume analysis revealed that while the slopes of the LV end-systolic pressure–volume relationship and preload recruitable stroke work (E_{es} and M_{PRSW}, respectively) remained normal, there were statistically significant

increases in the respective volume-axis intercepts (V_o and M_o) in the group with heart failure and preserved EF and dP/dt_{max}. Such shifts are indicative of reductions of chamber contractile strength [12] which are not evident from measurements of EF or dP/dt_{max}. Parallel shifts of the ESPVR towards larger volumes have been shown to occur in the setting of acute regional ischemia [18] but this is the first investigation of this phenomenon in setting of chronic regional myocardial infarction. Inability of echocardiography to detect a reduction in ejection fraction could also be due to the somewhat more limited accuracy and reproducibility of this technique compared to sonomicrometry.

From a hemodynamic point of view it was of interest to note that the shifts of ESPVR were comparable in the group of animals that exhibited HFPEF and those assigned to the SHF group, suggesting comparable effects on intrinsic ventricular systolic properties. This observation leads to the hypothesis that the difference between groups may reside in the vascular afterload. This was indeed confirmed by analysis of the effective arterial elastance (E_a, a pressure–volume-based index of arterial resistance). In animals in the HFPEF group, E_a decreased following development of heart failure, whereas it was maintained in the group that showed a reduction in ejection fraction. The reduction in E_a in the face of reduced ventricular function provided offsetting effects that allowed preservation of ejection fraction.

Histologic examination of tissue derived from the hearts revealed replacement fibrosis that was expected to cause increased regional myocardial stiffness and contribute to diastolic dysfunction [3]. The actual functional consequences were assessed through extensive analysis of ventricular EDPVRs. The induction of heart failure was not associated with a consistent shift of the EDPVR; in some hearts it shifted upward/leftward, in some it was unchanged and in others in was shifted downward/rightward. In all cases, because of higher filling pressures, the end-diastolic pressure–volume point resided on a steeper portion of the nonlinear EDPVR. Chamber stiffness constant was increased at the onset of heart failure state and returned to baseline during the follow-up period. There was no significant relationship between the value of chamber stiffness constant and end-diastolic pressure (Fig. 7). There was no change at any time point in myocardial chamber stiffness constant.

We propose that the mechanism by which heart failure (i.e., elevated EDP) develops in this model relates to neurohormonal activation. When systolic ventricular contractile strength is minimally compromised by small amounts of coronary microembolization, neurohormonal activation occurs. This may enhance myocardial performance to such a degree that EF and dP/dt_{max} can be maintained, even though more sensitive measures (e.g., ESPVR) are still able to detect a decrement in contractile function. Activation of neurohormonal mechanisms are known to lead to multiple effects, including renal salt and water retention (increased intravascular volume) [19], venoconstriction and volume redistribution from the peripheral to central compartments [20] which ultimately results in elevation of pulmonary venous pressure [21]. In this regard, the mechanism by which HF is induced and pulmonary venous pressures rise in these animals is likely to be similar to those responsible for these phenomena in systolic HF.

Coronary artery disease and prior myocardial infarction, conditions of myocardial dysfunction, myocyte loss and myocardial fibrosis, are commonly found in patients with heart failure and normal ejection fraction. Hellermann et al. found that approximately 30% of patients who developed heart failure following a myocardial infarction had preserved systolic function, defined as ejection fraction $\geq 50\%$ [2]. We propose that the animals described in this study may mimic heart failure with preserved ejection fraction in the setting of prior infarct. Consistent with our notions, it was shown in a group of patients with the diagnosis of *diastolic heart failure* in which approximately half had coronary artery disease, that there was objective evidence of impaired left ventricular systolic function demonstrated by tissue Doppler imaging (TDI) [22]. In contrast, *diastolic heart failure* in the setting of hypertension and ventricular hypertrophy (neither of which is observed in the animals of this study) may reflect a different pathophysiological state not addressed by this model.

We performed physiologic measurements only with animals at rest. It is possible that during exertion with increased heart rate, diastolic function may worsen and be found to contribute to the abnormal hemodynamics. We find this unlikely in these animals. The time constant of relaxation in the heart failure state averaged only 28 ms. It has been shown that even with doubling of the time constant during exertion, these rates of relaxation are insufficient to impair the ability of the heart to fill or result in incomplete relaxation between beats. A recent study in patients with heart failure and normal ejection fraction in the setting of hypertensive hypertrophy showed that despite marked increases in time constant of relaxation, left ventricular volume was able to be increased during exertion [23].

Another potential limitation of the present study was that while LV chamber enlargement was detected in the hearts of HFPEF and SHF groups using sonomicrometry, it was not detected by echocardiography. It is well known that two dimensional echocardiographic measurements of cross sectional dimensions at one level do not necessarily correlate well with three dimensional measurement of chamber volume, especially when regional changes in chamber properties are induced, as in the present model. Furthermore, echocardiographic measurements made at different times have inherent variability due to the fact that it is impossible to return to the exact same slice and angle on repeated measurements. Due to such inherent variability, relatively large numbers of observations would be needed to detect relatively small changes in volumes such as observed in the present study. These limitations are not present with sono-

micrometry, a technique with which the crystals are fixed in place. Such problems are present and well recognized in the clinical setting as well.

In summary, we show that with limited myocardial injury, heart failure can occur with preserved ejection fraction. There was a lack of a consistent shift of the EDPVR or correlation between chamber stiffness constant and end-diastolic pressure, indicating that diastolic dysfunction was not a primary mechanism leading to heart failure in this setting. Histologic changes suggestive of increased myocardial stiffness were present, but were not sufficient by themselves to cause a consistent elevation of the EDPVR or increase the myocardial stiffness constant. Parallel shifts of the ESPVR and PRSW towards larger volumes reveal a degree of systolic dysfunction not detected by EF or dP/dt_{max}. The degree of systolic impairment present in these animals was sufficient to cause neurohormonal activation and fluid retention of a degree comparable to that identified in animals with more significant systolic dysfunction (reduced EF and/or dP/dt_{max}). Therefore, as in the animals with more overt systolic dysfunction, we propose that neurohormonal activation and fluid retention may be important mechanisms underlying the elevation of end-diastolic pressure without diastolic dysfunction. The clinical implications of these findings are that heart failure with normal ejection fraction need not always be due to diastolic dysfunction. Although a majority of the literature related to HFPEF focuses on diastolic dysfunction, we propose that advances in understanding and therapeutics will result if efforts are also made to study extra-cardiac causes of heart failure and if we recognize that HFPEF does not necessarily result from a single pathophysiologic mechanism.

References

[1] Devereux RB, Roman MJ, Liu JE, et al. Congestive heart failure despite normal left ventricular systolic function in a population-based sample: the Strong Heart Study. Am J Cardiol 2000;86:1090–6.

[2] Hellermann JP, Jacobsen SJ, Reeder GS, Lopez-Jimenez F, Weston SA, Roger VL. Heart failure after myocardial infarction: prevalence of preserved left ventricular systolic function in the community. Am Heart J 2003;154:742–8.

[3] Grossman W. Diastolic dysfunction and congestive heart failure. Circulation 1990;81:III1–7.

[4] Zile MR, Brutsaert DL. New concepts in diastolic dysfunction and diastolic heart failure: Part I. Diagnosis, prognosis, and measurements of diastolic function. Circulation 2002;105:1387–93.

[5] Zile MR, Brutsaert DL. New concepts in diastolic dysfunction and diastolic heart failure: Part II. Causal mechanisms and treatment. Circulation 2002;105:1503–8.

[6] Petrie MC, Caruana L, Berry C, McMurray JJ. "Diastolic heart failure" or heart failure caused by subtle left ventricular systolic dysfunction? Heart 2002;87:29–31.

[7] Yip G, Wang M, Zhang Y, Fung JWH, Ho PY, Sanderson JE. Left ventricular long axis function in diastolic heart failure is reduced in both diastole and systole: time for a redefinition? Heart 2002;87:121–5.

[8] Knecht M, Burkhoff D, Yi GH, et al. Coronary endothelial dysfunction precedes heart failure and reduction of coronary reserve in awake dogs. J Mol Cell Cardiol 1997;29:217–27.

[9] Sabbah HN, Stein PD, Kono T, et al. A canine model of chronic heart failure produced by multiple sequential coronary microembolizations. Am J Physiol 1991;260:H1379–84.

[10] Dubroff JM, Clark MB, Wong CY, Spotnitz AJ, Collins RH, Spotnitz HM. Left ventricular ejection fraction during cardiac surgery: a two-dimensional echocardiographic study. Circulation 1983;68:95–103.

[11] Sagawa K. The end-systolic pressure–volume relation of the ventricle: definition, modifications and clinical use. Circulation 1981;63:1223–7.

[12] Kass DA, Maughan WL. From 'Emax' to pressure–volume relations: a broader view. Circulation 1988;77:1203–12.

[13] Glower DD, Spratt JA, Snow ND, et al. Linearity of the Frank-Starling relationship in the intact heart: the concept of preload recruitable stroke work. Circulation 1985;71:994–1009.

[14] Mirsky I, Pasipoularides A. Clinical assessment of diastolic function. Prog Cardiovasc Dis 1990;32:291–318.

[15] Tomita M, Spinale FG, Crawford FA, Zile MR. Changes in left ventricular volume, mass, and function during the development and regression of supraventricular tachycardia-induced cardiomyopathy. Disparity between recovery of systolic versus diastolic function. Circulation 1991;83:635–44.

[16] Sunagawa K, Maughan WL, Burkhoff D, Sagawa K. Left ventricular interaction with arterial load studied in isolated canine ventricle. Am J Physiol 1983;245(HCP 14):H773–80.

[17] Feldschuh J, Enson Y. Prediction of the normal blood volume. Relation of blood volume to body habitus. Circulation 1977;56:605–12.

[18] Sunagawa K, Maughan WL, Sagawa K. Effect of regional ischemia on the left ventricular end-systolic pressure–volume relationship of isolated canine hearts. Circ Res 1983;52:170–8.

[19] Schrier RW, Abraham WT. Hormones and hemodynamics in heart failure. N Engl J Med 1999;341:577–85.

[20] Wang SY, Manyari DE, Scott-Douglas N, Smiseth OA, Smith ER, Tyberg JV. Splanchnic venous pressure–volume relation during experimental acute ischemic heart failure. Differential effects of hydralazine, enalaprilat, and nitroglycerin. Circulation 1995;91:1205–12.

[21] Burkhoff D, Tyberg JV. Why does pulmonary venous pressure rise following the onset of left ventricular dysfunction: a theoretical analysis. Am J Physiol 1993;265(HCP 34):H1819–28.

[22] Yu CM, Lin H, Yang H, Kong SL, Zhang Q, Lee SWL. Progression of systolic abnormalities in patients with "isolated" diastolic heart failure and diastolic dysfunction. Circulation 2002;105:1195–201.

[23] Kawaguchi M, Hay I, Fetics B, Kass DA. Combined ventricular systolic and arterial stiffening in patients with heart failure and preserved ejection fraction: implications for systolic and diastolic reserve limitations. Circulation 2003;107:714–20.